ADVANCES IN ATMOSPHERIC SCIENCES, VOL. 25, NO. 1, 2008, 31–42

Simulation of Terrestrial Dust Devil Patterns

GU Zhaolin*[1] (顾兆林), QIU Jian[2] (邱 剑), ZHAO Yongzhi[3] (赵永志), and LI Yun[2] (李 云)

[1] *Department of Environmental Science and Technology, School of Human Settlements and Civil Engineering, Xi'an Jiaotong University, Xi'an* 710049

[2] *School of Energy and Power Engineering, Xi'an Jiaotong University, Xi'an* 710049

[3] *Department of Chemical Engineering, Tsinghua University, Beijing* 100084

(Received 12 June 2006; revised 29 September 2007)

ABSTRACT

Introducing the surface properties [initial vortex, ground temperature and surface momentum impact height (SMIH)] for the boundary conditions, dust-devil-scale large eddy simulations (LES) were carried out. Given three parameters of initial vortex, ground temperature and the SMIH based on Sinclair's observation, the dust devil physical characteristics, such as maximum tangential velocity, updraft velocity, pressure drop in the inner core region, and even reverse flow at the top of the core region, are predicted, and are found to be close to the observations, thus demonstrating the ability of the simulation. The physical characteristics of different modeled dust devils are reproduced and compared to the values predicted by Renno et al.' theory. Even for smaller temperature differences or weaker buoyancy, severe dust devils may be formed by strong incipient vortices. It is also indicated that SMIH substantially affects the near-surface shape of terrestrial dust devils.

Key words: dust devil, dust storm, large eddy simulation (LES)

DOI: 10.1007/s00376-008-0031-7

1. Introduction

Dust is a main component of atmospheric aerosols. With several special wind systems, such as dust storms, dust devils etc., the mineral dust particles originate mainly from the great desert areas of northern Africa, Southwest America, and Asia. Mineral aerosols play a key role in atmospheric chemistry, ecology, and the Earth's radiative balance (Wang et al., 2004; Shen et al., 2006).

With a low pressure and a warm core, dust devils are vertical vortices that occur in the atmosphere's convective boundary layer (CBL), usually short in duration. Dust devils can swirl dust, debris and sand to high levels. They are concentrated vortices, occurring on various surfaces of the Earth (Vatistas et al., 1991). Their frequent appearance in some areas suggests that they are significant in the evolution of dust storms (Greeley et al., 2003). However, this is so far only speculation, without direct observational evidence (Cantor et al., 2002). Dust devils may arise from rising plumes in the CBL (e.g., Battan, 1958; Ryan and Carroll, 1970; Cortese and Balachandar, 1993; Shapiro and Kogan, 1994; Renno et al., 1998; Michaels and Rafkin, 2004) called "swirling rising plumes" (SRPs) (Zhao et al., 2004). There is a super-adiabatic lapse rate near the ground surface, which is the driving force for dust devils. Near the surface, warm air parcels spiral toward the centre while absorbing heat from the surface. The radial inflow of warm air into the rising plume results in the concentration of ambient vorticity.

Typical observed diameters of dust devils may depend strongly on geography. For Arizona dust devils, an average diameter is likely to be in the order of tens of meters (Sinclair, 1973). The heights of dust columns in dust devils are usually less than 600 m but, in desert conditions with deep mixed layers, and the thermal updrafts associated with them have been observed to extend as high as 4500 m (Sinclair, 1966). Renno et al. (1998) proposed a thermodynamic theory of dust devils and presented a range of thermodynamic parameters against Sinclair's (1966) observations.

*Corresponding author: GU Zhaolin, guzhaoln@mail.xjtu.edu.cn

Leovy (2003) pointed out that computer simulations have the potential to be an important tool for interpreting laboratory and field observations of dust devils. Computer flow simulations have been performed to gain insight into the dynamics of boundary layer vortices. In a laboratory simulation of turbulent convection, Willis and Deardorff (1979) found that dust-devil-like vortices were most likely to occur at the vertices of the cellular convective pattern, where vertical velocity reached its peak.

Kanak et al. (2000) found the existence of vertical vortices in the CBL by means of large eddy simulation (LES). Their model used a 35-m horizontal grid spacing, which is approximately the average diameter of extra-large dust devils, and may be classified as a CBL-scale model. Although this model could simulate the initiation of weak vertical vortices of dust devils, it cannot be used to study the fine flow structure, or the influence of surface and atmospheric parameters on dust devils. Therefore, smaller scale models are needed to solve these problems. In Kanak's recent work (2005), a high-resolution (2-m grid spacing) LES of the CBL was performed in order to examine the physical characteristics of dust-devil-scale vortices. Although the general features of the simulated dust-devil-like vortices agreed well with observations, the model was limited in a number of aspects, such as the pressure drop inside the simulated vortex core was not as great as observed, and the simulated vortex wind speeds were less than 10 m s^{-1}. It was also suggested that initial conditions of the simulation might have an important influence on the formation of vertical vortices.

Zhao et al. (2004) compared a CBL-scale simulation for convection cells with a dust-devil-scale simulation for the air flow of dust devils and found that, given appropriate initial conditions, such as heat flux and initial temperature field, the convection cell could be initiated, and thus easily allowing the development of air flow for dust devils. Different states of convection take different amounts of time to develop dust devil air flow fields. A three-dimensional, unsteady, high resolution model is presented to investigate the air flow evolution of a modeled dust devil, using fine grids—the radial grid spacing smoothly stretched from 0.1 m at the center to 4 m, and the vertical grid spacing stretched from 0.1 m on the surface to around 10 m at the top. Smagorinsky's (1963) scheme was used for parameterization of the sub-grid viscosity. This model might be a dust-devil-scale model. The simulation results show the air flow shape of dust devils, which are strongly affected by ground surface friction.

Many studies have shown that on a small scale, the shape and intensity of dust devils are sensitive to many factors, such as soil cover, physical characteristics, composition, topographical features, and weather (Renno et al., 2004). Based on the dust-devil-scale quasi-steady LES mathematical model, the present study aims to reproduce a variety of observed dust devil shapes by adjusting three key parameters, namely the incipient vortex, SMIH (surface momentum impact height), and ground surface temperature. The quasi-steady LES model and the choice of three parameters for boundary conditions are described in section 2. The air flow field of a modeled dust devil is simulated and analyzed in section 3. Six cases of modeled dust devils are reproduced in section 4 and compared with Renno et al. (1998) thermodynamic theory of dust devils. A summary is given in section 5.

2. LES model and boundary conditions

Figure 1 shows several kinds of terrestrial dust devils observed on different surfaces, e.g., bushes, shrub layers, deserts, and even airfields. The typical upside-down cone-like dust devil is common in nature. The dust devil with spray—regular dust cylinder in the inner core with sprays of flat, upside-down cone shapes near the ground—might have high tangential velocity and near-bottom momentum roughness. Bowl-like dust devils occur on smooth ground. The inflow air layer near the ground is very thin, and the bottom of the dust devil is relatively flat. If the ground is very smooth (such as in airports near deserts), no obvious draught spirals out, and the dust devil has a regular column shape. With a low pressure inner core and swirling plume, dust particles might become airborne, making the dust devil vortex visible if the surface is composed of loose material.

It follows from the dust devil images in Fig. 1 that the evolution, shape and intensity of dust devils may depend on surface properties, which might be present within the boundary conditions and initial conditions in the current simulation. In the following paragraphs, the three parameters (background vorticity, momentum roughness and ground temperature) are justified as the surface properties.

A number of investigators have proposed or provided evidence that larger scale convective circulations, that are not initially rotational, can provide vertical and/or tilted horizontal vorticity (e.g., Ryan and Carroll, 1970; Cortese and Balachandar, 1993; Shapiro and Kogan, 1994; Shapiro and Kanak, 2002; Michaels and Rafkin, 2004; Kanak, 2005). The vortex size of a dust devil is proportional to the value of the background vorticity (Renno and Bluestein, 2001). Hence, in dust-devil-scale simulation, the background vorticity, or incipient vortex, could be selected as a param-

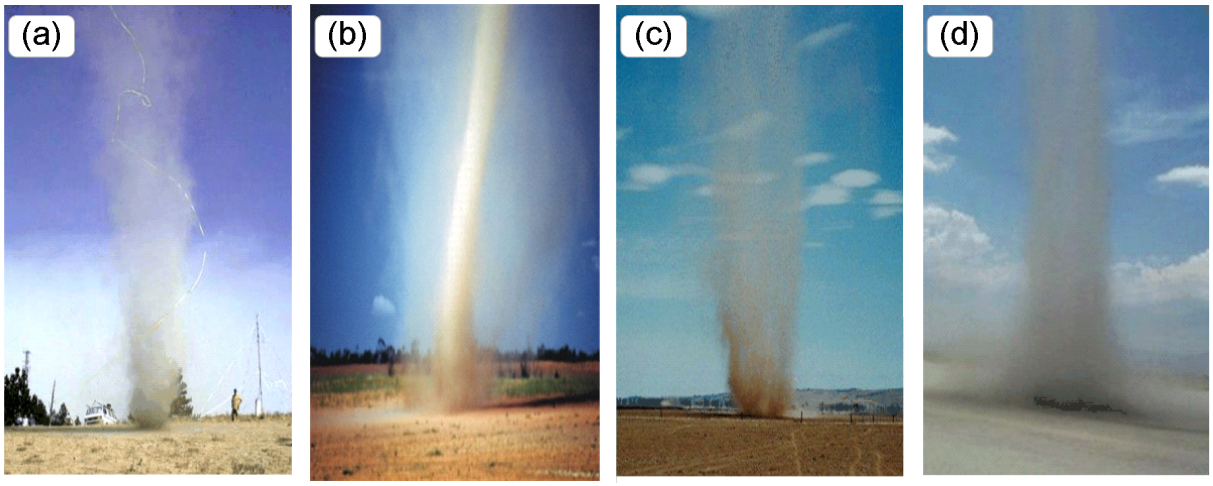

Fig. 1. Patterns of terrestrial dust devils. Image sources: (a) http://www.aeriane.com/images/; (b) http://www.inflowimages.com/code/showimage.asp?img=../chasereports/dustdevils/dd3.jpg; (c) http://www.saweather.net/photographs/vortex/; (d) http://www.weatherpictureoftheday.com/.

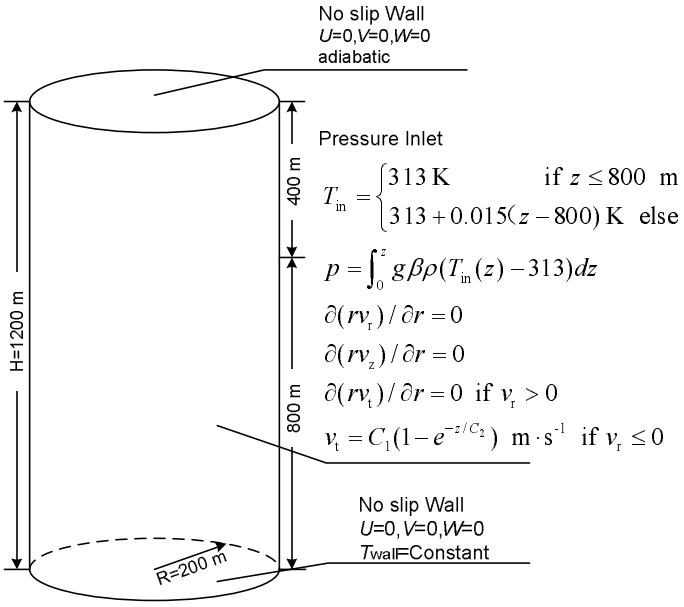

Fig. 2. Computational domain, initial and boundary conditions.

eter, expressed in terms of the tangential velocity on the boundary of the convection cell. The diameters of the convection cells are several hundreds of meters (Zhao et al., 2004).

The profiles of temperature, pressure, and the three cylindrical components of wind velocity through the base of a dust devil were measured near Tucson, Arizona (Sinclair, 1973). It follows from the observations of this study that the ambient air temperature is about 315 K. Furthermore, at different altitudes, $h = 5.2$ m and $h = 9.4$ m (V7 in 7 feet level and V31 in 31 feet level in the literature), the value of tangential velocities at $r = 50$ m, far from the dust devil center, is different. The tangential velocity at 9.4 m above the surface, 3.0 m s^{-1}, is obviously greater than that at 5.2 m, 1.5 m s^{-1}. This result could be explained by the friction of the surface (resulting from grass, sand, bush etc.) slows down the near-surface angular momentum. The momentum roughness is sensitive to the effect of friction, and thus the vertical distribution of the near-surface tangential velocity on the domain boundary (Leslie and Smith, 1977).

In light of the recorded profiles of tangential velocity beyond the center of the dust devil (Sinclair,

1966), a tangential velocity profile depicted by Eq. (1) is adopted for the background vorticity perturbation at the lateral boundary of the computational domain.

$$v_t(z) = C_1(1 - e^{-z/C_2}) \,, \tag{1}$$

where C_1 is the initial tangential velocity (rotating speed), representative of the background vorticity, and C_2 reflects the vertical distribution of the rotating speed, accounting for the influence of surface roughness on the near-ground flow. Different from the surface roughness, C_2 could be defined as the SMIH. Nevertheless, the SMIH is sensitive and directly proportional to the surface roughness.

Generally, a constant heat flux is specified on the surface (Kanak, 2005; Zhao et al., 2004) in the simulation models to allow for the buoyancy, or superadiabatic lapse rate, near the ground surface. Since the temperature difference between the ground surface and near-surface air parcels, causing convection, is related to the heat flux (Renno et al., 2004), the ground surface temperature might be considered as a key parameter that plays a significant role in determining the intensity of the updraft in the current LES model, when keeping the constant temperature of the converging ambient air parcels.

In summary, introducing incipient vortex, SMIH and surface temperature as the parameters of surface properties, the boundary conditions are described in Fig. 2. The diameter of the computational domain is 200 m, the same order of the diameter of heat convection cells.

Assuming the Boussinesq approximation is valid, and applying the filter of the Navier-Stokes equations for an incompressible buoyancy flow, the continuity Eq. (2), momentum Eq. (3) and energy Eq. (4) equations become:

$$\frac{\partial \bar{u}_j}{\partial x_j} = 0 \,, \tag{2}$$

$$\rho\frac{\partial \bar{u}_i}{\partial t} + \rho\frac{\partial(\bar{u}_i \cdot \bar{u}_j)}{\partial x_j} = -\frac{\partial \overline{P}}{\partial x_i} + \frac{\partial}{\partial x_j}\left[(\mu + \mu_{\mathrm{SGS}})\left(\frac{\partial \bar{u}_i}{\partial x_j} + \frac{\partial \bar{u}_j}{\partial x_i}\right)\right] + g\beta\rho(\overline{T} - T_c)\delta_{i3} \,, \tag{3}$$

$$\rho\frac{\partial \bar{e}}{\partial t} + \rho\frac{\partial(\bar{u}_j\bar{e})}{\partial x_j} = \frac{\partial}{\partial x_j}\left[\left(\frac{\mu}{Pr} + \frac{\mu_{\mathrm{SGS}}}{Pr_{\mathrm{SGS}}}\right)\frac{\partial \bar{e}}{\partial x_j}\right] \,, \tag{4}$$

where the overbar represents spatial filtering; ρ is the reference air density; u_i the velocity component; p the pressure; μ the viscosity; g the gravitational acceleration; Pr the Prandtl number; e the internal energy; β the thermal expansion coefficient; T_c the buoyancy reference temperature; and T the temperature. P is a modified pressure quantity containing both p and a kinetic energy term (Gu et al., 2006). δ_{i3} is the sum sign and is valued 1 when $i = 3$.

In the momentum and energy equations, the sub-grid viscosity requires specification in simulations. The SGS viscosity μ_{SGS} is:

$$\mu_{\mathrm{SGS}} = \rho C\bar{\Delta}^2|\overline{S}| \,, \tag{5}$$

where

$$|\overline{S}| = (2\overline{S}_{ij}\overline{S}_{ij})^{1/2}$$

is the magnitude of the resolved-scale rate-of-strain tensor. $\bar{\Delta}$ is the grid size. $\bar{\Delta} = V^{1/3}$ is usually employed. The coefficient C is determined by the dynamic sub-grid scale (SGS) model (Lilly, 1992). SGS Prandtl number Pr_{SGS} is taken as 0.33 (Nieuwstadt et al., 1991).

The air flow evolution of dust devil simulation is a transient problem; the initial conditions must be set to get the convection field. The initial radial and vertical velocities in the domain are set to zero and the initial field temperature up to 800 m is given, 313 K. The region above 800 m is preset as the inversion layer, in order to buffer the violent updraft. The field temperature T_{in} of the inversion layer above 800 m is given by $T_{\mathrm{in}} = 313 + 0.015\,(z - 800)$, units: K. At the same time, a weak vertical vortex (Ossen vortex; Green, 1995) is given in the initial vertical velocity field of the whole computational domain as the perturbation to ensure the flow reaching the quasi-steady state as soon as possible.

$$v_t = \frac{200C_1}{r}(1 - e^{-r^2/r_0^2})(1 - e^{-z/C_2}) \,, \tag{6}$$

where r is the distance from the centerline, $r_0 = 60$ m.

Details of the LES model, boundary and initial conditions can be referred to in the literature (Zhao et al., 2004; Gu et al., 2006). The fine grid points are adopted in the so-called dust-devil-scale model. In the computational domain, 200 m (R)×1200 m (H), 1008000, 80(r)×72(θ)×175(z), non-uniformly distributed grid points are used. The grid spacing is fixed for the azimuthal angle coordinate, while the radial grid spacing stretched from 0.1 m at the center to 5 m on the lateral boundary, and the vertical grid spacing stretched from 0.1 m on the surface to around 15 m at the domain top. The time step is Δt=0.02 s. Thus, a three-dimensional simulation (x, y, z) is performed based on the arrangement of the grid points, using a Cartesian coordinate system for the cylindrical computational domain.

Although the velocities are written in two forms, (u, v, w) referred to a Cartesian coordinate system and

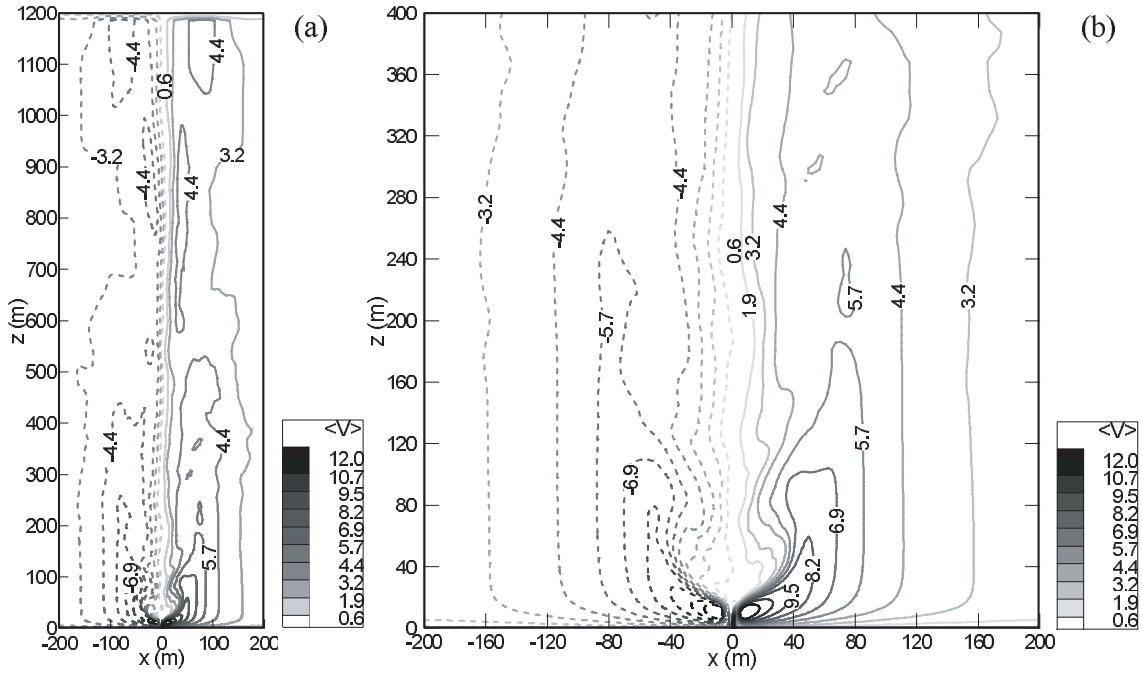

Fig. 3. Rotating speed (m s^{-1}) contours of the modeled dust devil with $T_{\rm wall}$=343 K, C_1=2.5 m s^{-1}, C_2=4.0 m. (a) The whole field. (b) The enlarged near-surface region. Dashed lines represent negative values.

$(v_{\rm r}, v_{\rm t}, v_{\rm z})$ referred to a cylindrical coordinate system, the simulated results are shown in a Cartesian coordinate system in this work, and then all the analysis is carried out.

3. Simulation of a modeled dust devil

Although the evolution of dust devils was divided into three stages (developing, developed and decaying) by Zhao et al. (2004), the mature phase—transition from the developed stage to the decaying stage, lasting several minutes to tens of minutes—is focused on in this paper. In the current LES model and algorithm, it takes about 200 s for the atmosphere flow of dust devil to reach the quasi-steady state. The quasi-steady state of the air flow field of the modeled dust devil means that the time-averaged air flow field does not change; for example, the time-averaged air flow field within 30 s is similar to the time-averaged air flow field within 60 s. This quasi-steady state indicates the characteristics of the gas phase field in the mature phase of modeled dust devils (Gu et al., 2006). Simulation results averaged every 30 s are shown in Figs. 3–7 for the present study.

The wind velocity is composed of the velocity in the vertical plane (denoted as v_z, or W), the radial velocity (denoted as $v_{\rm r}$, or U) and the tangential velocity (rotating speed) (denoted as $v_{\rm t}$, or V) on the horizontal plane, among which the tangential velocity is the key parameter in describing the shape of dust devils. The maximum rotating speed, the maximum updraft speed, and the pressure drop in the inner core of dust devils in the developed stage are, generally, used to indicate the intensity of dust devils.

Based on the observations by Sinclair (1973), the initial tangential velocity (background vorticity), C_1 = 2.5 m s^{-1}, and SMIH, C_2 = 4.0 m are selected for the boundary condition parameters in Eq. (1). The temperature difference is the main driving force for convection in dust devils. Li (2002) measured the distribution of air temperature over deserts and reported that the temperature difference between the ground and the air at a level of 1 m is over 20–30 K at midday in deserts. In the present simulation, the average atmospheric temperature at midday in deserts is assumed to be 313 K. A ground surface temperature of 343 K is used to provide a case with a large temperature difference or strong convection. The super-adiabatic lapse rate near the surface is thus evaluated by the temperature difference. The simulation results in the $y = 0$ slice are demonstrated in Figs. 3–6.

Figure 3a illustrates the tangential velocity contours in the entire computational domain and Fig. 3b gives the tangential velocity contours in the near-surface region. As shown in Fig. 3b, the flow of a fully developed dust devil vortex is divided into four

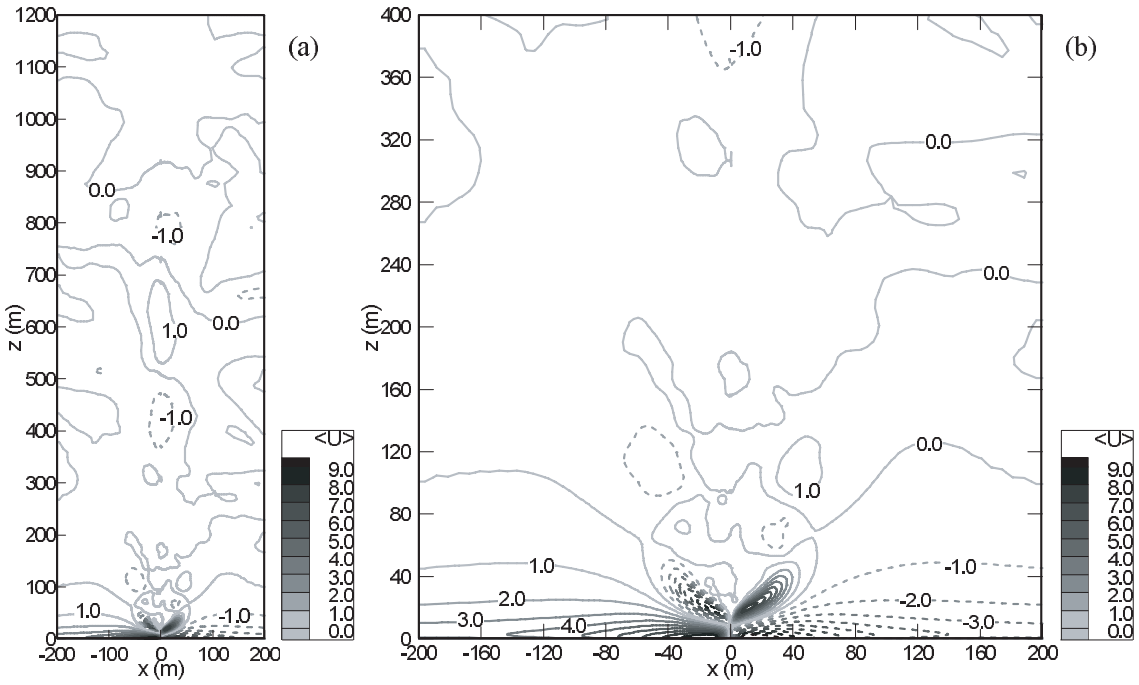

Fig. 4. Radial velocity (m s^{-1}) contours of the modeled dust devil with T_{wall}= 343 K, C_1=2.5 m s^{-1}, C_2=4.0 m. (a) The whole field. (b) The enlarged near-surface region. Dashed lines represent negative values.

regions: the outer flow region, the core region, the corner, and the near-surface layer (Zhao et al., 2004). The "core region" is the central core of the vortex. It is the mainstream of dust devils, where there is low pressure updraft in the inner core zone of the core region. The outer flow region is beyond the core region, where the air flow swirls slowly in response to the background vorticity and the positive buoyancy force in the convective plume. The inflow spirals into the center in near-surface or inflow layers, and then deflects upward into the corner region. The maximum tangential velocity in the corner region is about 12 m s^{-1}. This maximum tangential velocity contour consists of the core ring, whose radius is about 10 m in this case. The swirling velocity at a certain level, about 2.5 m, in the corner is much greater than in the "core region" above the corner. The highest swirling velocity and the strongest turbulence of an actual dust devil are generally located in the corner region (Sinclair, 1973; Hess and Spillane, 1990), showing that the present simulation results are acceptable.

Figure 4a demonstrates the radial velocity contours in the whole domain and Fig. 4b shows the radial velocity contours in the near-surface zone. The maximum radial velocity is about 10 m s^{-1}, which means there is a large wind shear in the near-surface layer. Figure 5a shows the whole field's vertical velocity contours and Fig. 5b shows the local vertical velocity contours in the near-surface. The maximum ascending velocity is about 16 m s^{-1}, occurring in the corner region near the surface. At the top of the inner core, the vortex breakdown (Snow, 1982), stagnant air parcels and even reverse flow, emerges in the mature phase. In the present simulation, there is a downdraft, occurring in the inner core over the corner region, with a maximum velocity of -3 m s^{-1}, as shown in Fig. 5. When the vortex breakdown reaches the ground surface, the dust devil overspreads markedly and enters into the decaying stage, lasting several minutes or longer.

Figure 6a shows the whole field's pressure drop contours and Fig. 6b shows the local pressure drop contours in the near-surface. It is demonstrated that higher swirling updraft results in higher pressure drops in the inner core of the dust devil, the maximum reaching 2 hPa. As discussed by Zhao et al. (2004), the pressure drop indicates the cyclostrophic balance between the centrifugal force and the radial pressure gradient in the mature stage.

The typical pressure drop observed within dust devils varies from 2.5 to 4.5 hPa (Sinclair, 1973). The near-surface vertical velocity reaches peak values of about 15 m s^{-1} (Ives, 1947; Sinclair, 1973). Weak thermal updrafts and small dust devils are frequently observed in the wake of large dust devils. The low-level tangential velocity also reaches peak values of about 15 m s^{-1}. The predicted dust devil physical charac-

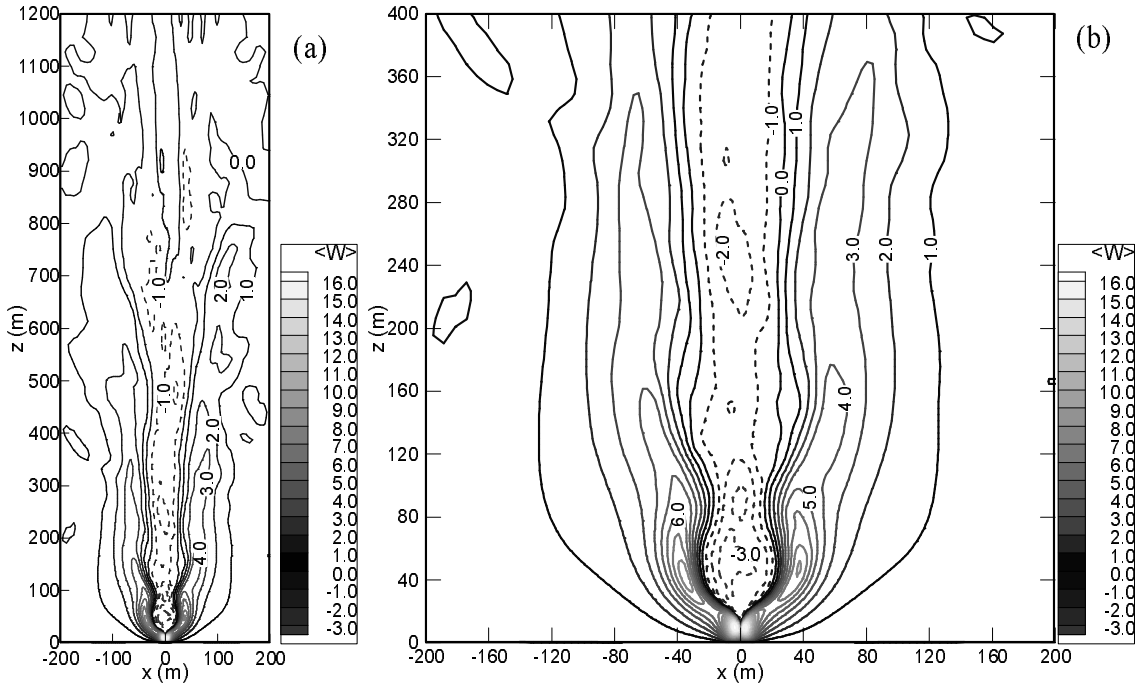

Fig. 5. Vertical velocity (m s^{-1}) contours of modeled dust devil with T_{wall}=343 K, C_1=2.5 m s^{-1}, C_2=4.0 m. (a) The whole field. (b) The enlarged near-surface region. Dashed lines represent negative values.

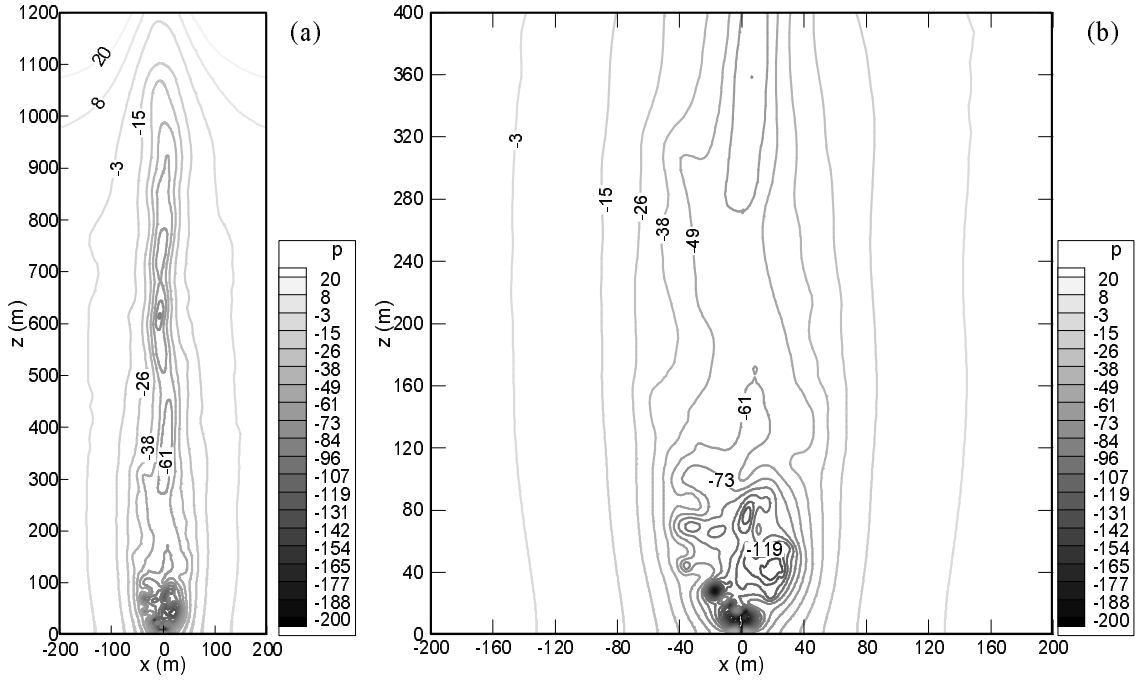

Fig. 6. Pressure drop (Pa) contours of the modeled dust devil with T_{wall}=343 K, C_1=2.5 m s^{-1}, C_2=4.0 m. (a) The whole field. (b) The enlarged near-surface region.

Table 1. Modeled dust devils and typical parameters.

Experiments	SMIH (m)	Ground temperature (K)	Initial vorticity (m s^{-1})	Maximum rotating and updraught speed, v and w, and pressure drop, Δp
A	4.0	343	2.5	$v = 12$ m s^{-1}, $w = 16$ m s^{-1}, Δp=2 hPa
B	4.0	343	5.0	$v = 20$ m s^{-1}, w=22 m s^{-1}, Δp=4.2 hPa
C	4.0	323	2.5	$v = 10$ m s^{-1}, w=10 m s^{-1}, Δp=1 hPa
D	4.0	323	5.0	$v = 18$ m s^{-1}, w=17 m s^{-1}, Δp=3.6 hPa
E	2.0	343	2.5	$v = 12$ m s^{-1}, w=9.5 m s^{-1}, Δp=3 hPa
F	6.0	343	2.5	$v = 16$ m s^{-1}, w=38 m s^{-1}, Δp=8.5 hPa

teristics, such as the maximum tangential velocity, the updraft velocity, the pressure drop in the inner core region, and even the reverse flow at the top of the core region, are close to the observations and thus demonstrate the ability of the present simulation.

4. Patterns of modeled terrestrial dust devils

By using different combinations of the incipient vortex, surface momentum impact height and surface temperature for different surfaces, a variety of flow patterns of modeled terrestrial dust devils in the developed stage have been reproduced to unveil the different shapes and intensities of dust devils in nature. The chosen values for the coefficients in Eq. (1) are given in Table 1. The rotating speed of the initial perturbed vertical vortex, C1, is the tangential velocity at the column boundary. Values of 2.5 m s^{-1} and 5.0 m s^{-1} are used to represent a weak initial vorticity and a strong initial vorticity, respectively. It is well known that dust devils can occur on different surfaces, such as bushes, shrub layers, deserts, and even airfields. Therefore, different values are selected to simulate three levels of SMIH.

Temperature difference is the main driving force for convection in dust devils. A surface temperature of 323 K is adopted in the cases of small temperature difference or weak convection.

The rotating velocity contours in the mature phase of modeled dust devils at different parametric conditions are presented in Figs. 7a–f. For a moderate SMIH, 4.0 m, a weak initial vorticity (initial rotating speed, 2.5 m s^{-1}) and a strong convection (surface temperature, 343 K), the near-surface shape of the modeled dust devil resembles an upside-down cone, which is illustrated schematically in Fig. 8a. As mentioned in section 3, there is an updraft with a maximum velocity up to 16 m s^{-1} in the corner region, while the maximum rotating velocity in the core is 12 m s^{-1} and the maximum radial velocity is 10 m s^{-1}. The pressure drop in the inner core is about 2 hPa (Model A in Table 1).

If the surface momentum impact height and temperature difference are kept the same as those of Model A, an increase of C_1 to 5.0 m s^{-1} results in the dramatic increase of the maximum rotating speed of the dust devil, up to 20 m s^{-1}, and the pressure drop in the inner core, reaching 4.2 hPa (Model B in Table 1). The cone angle of the upside-down cone is widened and the near-surface shape of the dust devil becomes flat (Fig. 7b). When the convection becomes weaker, e.g., at a surface temperature of 323 K, while keeping the same surface momentum impact height and initial rotating speed, the predicted near-surface rotating speed and updraft velocity are the same value, 10 m s^{-1}, which is accompanied by a reduction in pressure drop in the inner core, 1 hPa (Model C in Table 1 and Fig. 7c).

A modeled dust devil with a moderate momentum roughness of 4.0 m, a strong initial vorticity (initial rotating speed, 5.0 m s^{-1}) and a weak convection (surface temperature, 323 K) is shown in Fig. 7d. An almost regular and cylindrical vortex is found in the core region, whilst there exists a second upside-down cone, which is low and flat, due to the dust-laden overflow in the corner region (referring to Fig. 1b). This modeled dust devil looks like a cylindrical vertical vortex with an upside-down conic airborne dust spout near the ground (Fig. 8b). This type of dust devil has a high rotating velocity and is likely to be quite severe. In this case, the maximum updraft velocity and the maximum rotating velocity in the corner region are 17 m s^{-1} and 18 m s^{-1}, respectively, while the pressure depression in the inner core is up to 3.6 hPa (Model D in Table 1).

The modeled dust devil shown in Fig. 7e has half the SMIH as compared to the case in Fig. 7a. The maximum updraft velocity is low, down to 9.5 m s^{-1}, while the maximum rotating velocity in the corner region keeps the same value, 12 m s^{-1}. The pressure drop in the inner core is 3 hPa (Model E in Table 1). This type of dust devil is clearly different from those described above, and has a bowl shape in the near-surface region, as shown in Fig. 8c. It is likely to occur in places with a flat and smooth surface, where the SMIH is very small, so that there is no obvious spiraling outward overflow. For a smooth surface, the

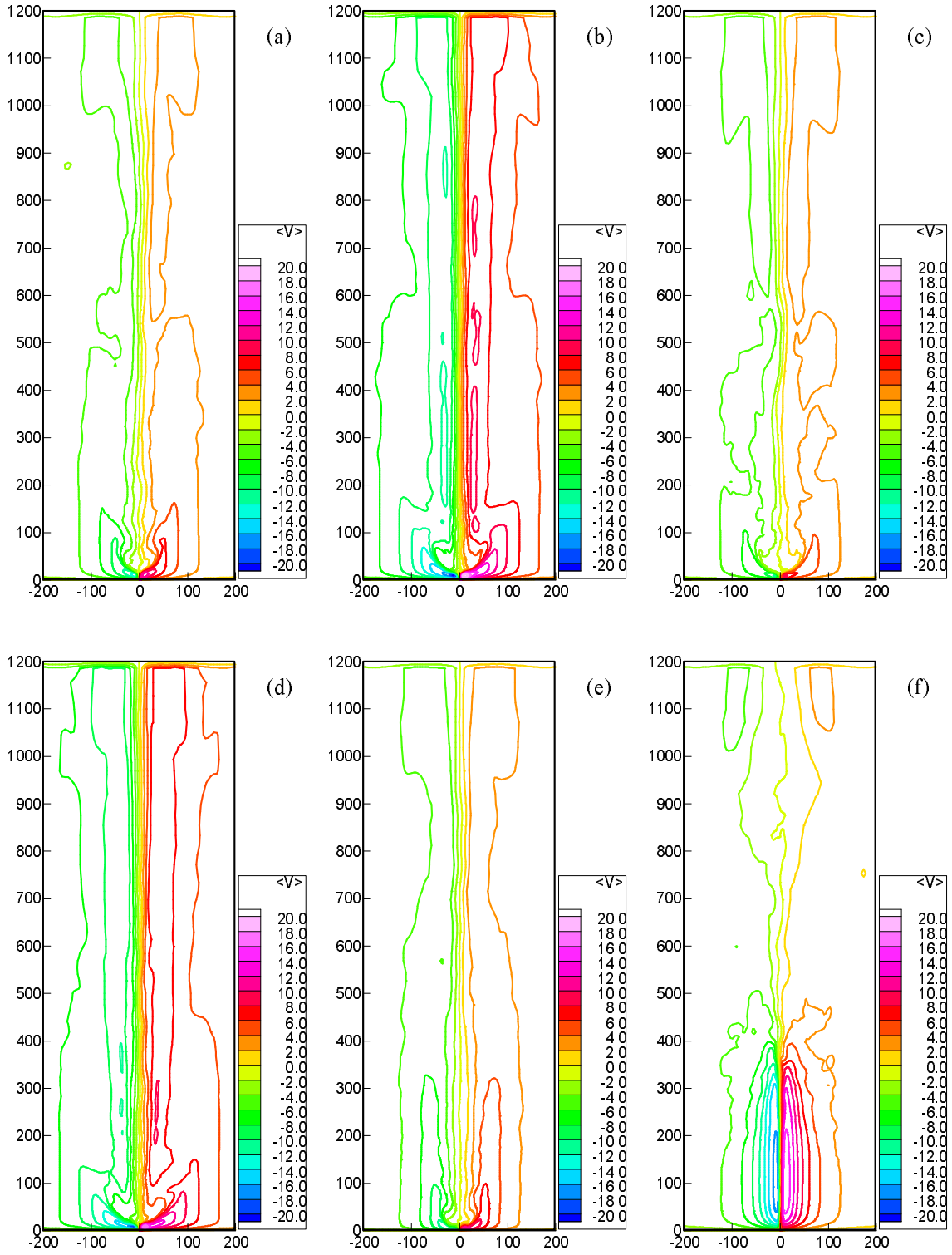

Fig. 7. Rotating velocity contours in the mature phase of modeled dust devils, m s^{-1}, in the $x - z$ plane. The velocity is the time-averaging value. (a) moderate momentum roughness, weak vorticity and strong convection; (b) moderate momentum roughness, strong vorticity and strong convection; (c) moderate momentum roughness, weak vorticity and weak convection; (d) moderate momentum roughness, strong vorticity and weak convection; (e) small momentum roughness, weak vorticity and strong convection; and (f) large momentum roughness, weak vorticity and strong convection.

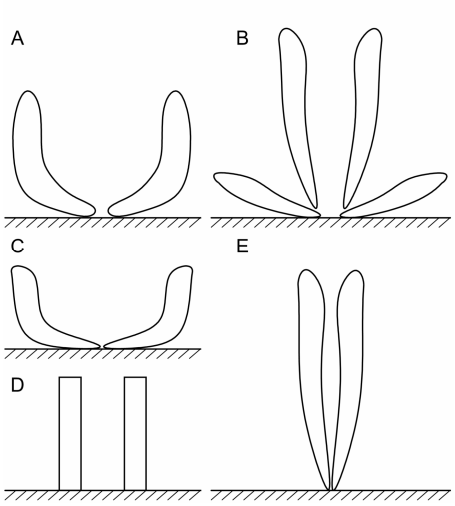

Fig. 8. Near-surface shapes of dust devils simplified by the periphery of the rotating velocity contour of their cores. (A) Upside-down cone-like dust devil. (B) Almost cylindrical vortex core surrounded by an upside-down cone-like dust spray. (C) Upside-down cone-like dust devil with enlarged cone. (D) Regular cylinder-like dust devil. (E) Upside-down thin cone-like dust devil with very small cone.

air parcels in the convergence layer spirals in a laminar way, and the shape of the dust devil resembles a regular cylinder (Fig. 8d). The shear stress near the ground surface is small and thus the vertical distribution of rotating speeds near the ground changes little. The radial converging speed varies slightly along the vertical direction.

The modeled dust devil with the largest surface momentum impact height, 6.0 m, is shown in Fig. 7f. It has a shape of a thin upside-down cone with a very small conic angle (Fig. 8e). Almost all the high temperature region lies in the core. There is a strong updraft with a maximum velocity up to 38 m s^{-1} in the corner region, while the maximum rotating velocity in the core is 16 m s^{-1} and the maximum radial velocity is 9 m s^{-1} (Model F in Table 1). Owing to high SMIH, the low vorticity layer near the ground is thick. The pressure drop in the inner core, approximately 8.5 hPa, is the highest among all the modeled dust devils.

Renno et al. (1998) proposed a thermodynamic theory of dust devils, based on the heat engine framework. This theory provides a simple physical interpretation for many of the observed characteristics of dust devils. Using the theory in our modeled dust devils and assuming $\overline{T}_S \approx T_H \approx T_\infty = 320$ K, T_0=340 K, $p_S \approx p_\infty \approx 1000$ hPa, $p_{top} \approx 860$ hPa, we obtain $\eta \approx 0.02$, $\eta_H \approx 0.062$. For dry air, let c_p=1005 J kg^{-1} K^{-1}, $\chi \approx 0.286$, and $\gamma \approx 0.5 \sim 1.0$, allowing us to obtain $v \approx$ 14–20 m s^{-1}, and $\Delta p \approx$2.0–4.6 hPa. Although the temperature perturbation is a bit different from the effective temperature perturbation presented by Renno et al. (2004), most values of the maximum tangential velocity and pressure drop in our modeled dust devils are close to the range predicted by Renno et al. (2004), hence supporting the current simulations.

In addition, these values of maximum tangential velocity, maximum updraft velocity and pressure drop in modeled dust devils approach the values observed by Sinclair (1973). Model F is an exception. The momentum thickness in the modeled dust devil shown in Fig. 7f might be too great to achieve simulation results far from Renno et al. (2004) and the observations. However, it is interesting to demonstrate the influence of SMIH.

The interconnection of the surface properties and the column shape of dust devils are investigated based on the dust-devil-scale LES model. It is indicated that the SMIH substantially affects the shape of terrestrial dust devils, changing from a column on a very smooth surface (Fig. 8d), an upside-down cone-like dust devil near the ground, a bowl-like dust devil on the surface with small SMIH (Fig. 8c), to an upside-down thin cone-like dust devil with a very small cone angle on the surface with large SMIH (Fig. 8e), whilst the intensity of dust devils increases with a decrease in conic angle. Even for a smaller temperature difference, severe dust devils may be formed by strong incipient vortices (Fig. 4b).

5. Summary

A dust-devil-scale LES model has been briefly described in this paper. Introducing the initial vortex, ground temperature and SMIH as the parameters of surface properties, the boundary conditions have been discussed. Although the evolution of dust devils was divided into three stages (developing, developed and decaying) by Zhao et al. (2004), the mature phase was the focus of this work. The wind velocity is composed of the velocity in the vertical plane, the radial velocity and the tangential velocity (rotating speed) on the horizontal plane. The maximum rotating speed, the maximum updraft speed, and the pressure drop in the inner core of dust devils in the mature phase could be employed to indicate the intensity of dust devils.

Given three parameters of initial vortex, ground temperature and momentum roughness based on Sinclair's (1966) observation, dust devil physical characteristics, such as maximum tangential velocity, updraft velocity, pressure drop in the inner core region, and even reverse flow at the top of the core region, were predicted, with the results approaching observations and thus demonstrating the ability of the sim-

ulation. Although the temperature perturbation was a bit different from the effective temperature perturbation presented by Renno et al. (1998), most values of the maximum tangential velocity and pressure drop in our modeled dust devils were close to their results. Thus, given the surface properties, the pressure drop and wind velocity of dust devils could be simulated.

Even for smaller temperature differences—weaker buoyancy, severe dust devils may be formed by strong incipient vortices. It is indicated that the SMIH substantially affects the near-surface shape of terrestrial dust devils, changing from a column on a very smooth surface to an upside-down cone-like dust devil near the ground. Different SMIH results in different conic angles. The tangential velocity, and hence intensity of the dust devil, increases with a decrease in conic angle.

Acknowledgements. The authors would like to thank the two anonymous reviewers for their suggestions and helpful criticisms, which helped to substantially improve the paper. This work was supported by the National Natural Science Foundation of China (Grant No. 40675011), the Chinese National Key Project of Basic Research (Grant Nos. 2004CB720208 and 2003CCC01500), and the Trans-century Training Program Foundation for Talents by the Ministry of Education of China. The authors also appreciate the support of Key Laboratory of Mechanics on Disaster and Environment in Western China (Lanzhou University), Ministry of Education.

REFERENCES

Battan, L. J., 1958: Energy of a dust devil. *J. Meteor.*, **15**, 235–237.

Cantor, B., M. Malin, and K. S. Edgett, 2002: Multiyear Mars Orbiter Camera (MOC) observations of repeated Martian weather phenomena during the northern summer season. *J. Geophys. Res. E*, **107**(3), 5014, doi:10.1029/2001JE001588.

Cortese, T., and S. Balachandar, 1993: Vertical nature of thermal plumes in turbulent convection. *Physics of Fluids A*, **5**, 3226–3232.

Greeley, R., M. R. Balme, J. D. Iversen, S. Metzger, R. Mickelson, J. Phoreman, and B. White, 2003: Martian dust devils: Laboratory simulations of particle threshold. *J. Geophys. Res. E*, **108**(5), 7–1.

Green, S. I., 1995: *Fluid Vortices*. Kluwer Academic Publishers, Dordrecht, Netherlands, 878pp.

Gu, Z., Y. Zhao, Y. Li, Y. Yu, and X. Feng, 2006: Numerical simulation of dust lifting within dust devils-simulation of an intense vortex. *J. Atmos. Sci.*, **63**, 2630–2641.

Hess, G. D. and K. T. Spillane, 1990: Characteristics of dust devils in Australia. *J. Appl. Meteor.*, **29**, 498–507.

Ives, R. L. 1947: Behavior of dust devils. *Bull. Amer. Meteor. Soc.*, **28**, 168–174.

Kanak, K. M., 2005: Numerical simulation of dust devil-scale vortices. *Quart. J. Roy. Meteor. Soc.*, **131**, 1271–1292.

Kanak, K. M., D. K. Lilly, and J. T. Snow, 2000: The formation of vertical vortices in the convective boundary layer. *Quart. J. Roy. Meteor. Soc.*, **126**, 2789–2810.

Leslie, L. M., and R. K. Smith, 1977: On the choice of radial boundary conditions for numerical models of sub-synoptic vortex flows in the atmosphere, with application to dust devils. *Quart. J. Roy. Meteor. Soc.*, **103**, 499–510.

Leovy, C. B., 2003: The devil is in the dust. *Nature*, **424**(6952), 1008–1009.

Li, J. F., 2002: *Desert Climate*. China Meteorological Press, Beijing, 185pp. (in Chinese)

Lilly, D. K., 1992: A proposed modification of the Germano subgrid-scale closure method. *Physics of Fluids A*, **4**(3), 633–635.

Michaels, T. I., and S. C. R. Rafkin, 2004: Large eddy simulation of atmospheric convection on Mars. *Quart. J. Roy. Meteor. Soc.*, **130**(599), 1251–1274.

Nieuwstadt, F. T. M., M. Mason, J. P. Moeng, and U. Schumann, 1991: Large eddy simulation of the convection boundary layer: A comparison of four computer codes. *Proc. 8th Symposium on Turbulent Shear Flows*, Springer-Verlag, 651–664.

Renno, N. O., and H. B. Bluestein, 2001: A simple theory for waterspouts. *J. Atmos. Sci.*, **58**, 927–932.

Renno, N. O., M. L. Burkett, and M. P. Larkin, 1998: A simple thermodynamical theory for dust devils. *J. Atmos. Sci.*, **55**, 3244–3252.

Renno, N. O., and Coauthors, 2004: MATADOR 2002: A pilot field experiment on convective plumes and dust devils. *J. Geophys. Res. E*, **109**, 1–10.

Ryan, J. A., and I. J. Carroll, 1970: Dust devils wind velocities: Mature state. *J. Geophys. Res.*, **75**, 531–541.

Shapiro, A., and Y. Kogan, 1994: On vortex formation in multicell convective clouds in a shear-free environment. *Atmospheric Research*, **33**, 125–136.

Shapiro, A., and K. M. Kanak, 2002: Vortex formation in ellipsoidal thermal bubbles. *J. Atmos. Sci.*, **59**, 2253–2269.

Shen, Z., J. Cao, X. Li, T. Okuda, Y. Wang, and X. Zhang, 2006: Mass concentration and mineralogical characteristics of aerosol particle collected at Dunhuang during ACE-Asia. *Adv. Atmos. Sci.*, **23**(2), 291–298.

Sinclair, P. C., 1966: A quantitative analysis of the dust devil. Ph. D. dissertation, University of Arizona, 292pp.

Sinclair, P. C., 1973: The lower structure of dust devils. *J. Atmos. Sci.*, **30**, 1599–1619.

Smagorinsky, J., 1963: General circulation experiments with the primitive equations: Part I, The basic experiment. *Mon. Wea. Rev.*, **91**, 199–164.

Snow, J. T., 1982: A review of recent advances in tor-

nado vortex dynamics. *Rev. Geophys. Space Phys.*, **20**, 953–964.

Vatistas, G. H., V. Kozel, and W. C. Mih, 1991: Simpler model for concentrated vortices. *Experimental Fluids*, **11**, 73–76.

Wang, M., Q. Liu, and X. Yang, 2004: A review of research on human activity induced climate change I greenhouse gases and aerosols. *Adv. Atmos. Sci.*, **21**(3), 314–321.

Willis, G. E., and J. W. Deardorff, 1979: Laboratory observations of turbulent penetrative convection platforms. *J. Geophys. Res.*, **84**, 296–301.

Zhao, Y. Z., 2004: Large eddy simulation of dust devils. Ph. D. dissertation, Xi'an Jiaotong University, China, 160pp. (in Chinese)

Zhao, Y. Z., Z. L. Gu, Y. Z. Yu, Y. Ge, Y. Li, and X. Feng, 2004: Mechanism and large eddy simulation of dust devils. *Atmos.-Ocean*, **42**, 61–84.